

## A new dynamic k- $\epsilon$ subgrid scale model

F. GALLERANO, G. CANNATA, L. MELILLA  
Dipartimento di Idraulica Trasporti e Strade  
Università di Roma "La Sapienza"  
Via Eudossiana 18, Roma  
ITALY

*Abstract:* - A new LES model is proposed. The proposed closure relation for the generalized SGS turbulent stress tensor: complies with the principle of turbulent frame indifference; takes into account both the anisotropy of the turbulence velocity scales and turbulence length scales; removes any balance assumption between the production and dissipation of SGS turbulent kinetic energy. In the proposed model the generalized SGS turbulent stress tensor is related exclusively to the generalized SGS turbulent kinetic energy (which is calculated by means of its balance equation) and the modified Leonard tensor. The filtered momentum equations are solved by using a staggered fourth order finite difference scheme. The proposed model is tested for a turbulent channel flow at Reynolds numbers (based on friction velocity and channel half-width) ranging from 395 to 2340.

*Key-Words:* - LES, closure relation, k- $\epsilon$ , subgrid model

### 1 Introduction

Among the most common LES models present in literature are the Dynamic Smagorinsky-type SGS Models (e.g., Dynamic Smagorinsky Mode DSM [1], Dynamic Mixed Model DMM1 [2], DMM2 [3], Lagrangian Dynamic Model LDM [4], Dynamic Two-parameter Model DTM [5]), in which the generalized SGS turbulent stress tensor is related to the resolved strain-rate tensor by means of a scalar eddy viscosity. It is assumed in these models that the eddy viscosity is a scalar proportional to the cubic root of the generalized SGS turbulent kinetic energy dissipation and that such dissipation is locally and instantaneously balanced by the production of the generalized SGS turbulent kinetic energy (i.e., by the rate of kinetic energy per unit of mass transferred from the large scales, larger than the filter size, to the unresolved ones). Consequently, it is evident that the dynamic Smagorinsky-type SGS models are fraught with three relevant drawbacks. The first drawback is represented by the scalar definition of the eddy viscosity; the second one concerns the local balance assumption of the generalized SGS turbulent kinetic energy production and dissipation, whilst the third drawback is related to the dynamic calculation of the coefficient used to model the eddy viscosity (Smagorinsky coefficient).

The scalar definition (first inconsistency) of the eddy viscosity is equivalent to assuming that the principal axes of the generalized SGS turbulent stress tensor, or the unresolved part of it (represented by the cross and Reynolds terms), are aligned with the principal axes of the resolved strain-rate tensor. This assumption has been disproved by many experimental tests and by DNS, which demonstrate that there is no alignment between the generalized SGS turbulent stress tensor, or the unresolved part of it, and the resolved strain-rate tensor [6]. Moreover, the eddy viscosity

is proportional to the product of two terms, of which the dimensions are, respectively, those of a length and a velocity [7]. These terms, which represent, respectively, the turbulence length scales and turbulence velocity scales, are, more generally, second-order tensors of which the product is a fourth-order tensor which represents the eddy viscosity [8]. The scalar definition of the eddy viscosity, used in the above-mentioned dynamic Smagorinsky-type SGS models, presupposes the existence of a single turbulence velocity scale and a single turbulence length scale. This is equivalent to assuming that the second-order tensors which represent the turbulence length scales and the turbulence velocity scales are isotropic and that, therefore, the turbulence is isotropic. In this manner, the turbulence anisotropy induced by the continuous transfer of energy from the mean flow towards the turbulent fluctuations, which is generally extremely anisotropic, is not considered. Even though the energy cascade process causes a reduction of the turbulence anisotropy, many authors [9] demonstrated that even in the dissipation range of the smallest turbulent scales, where viscous dissipation occurs, there is a high anisotropy level even at high Reynolds numbers.

The second inconsistency of the Smagorinsky dynamic models is related to the assumption of a local and instantaneous balance between production and dissipation of the generalized SGS turbulent kinetic energy, formulated in the above-mentioned models to obtain the turbulent viscosity expression. This assumption is confirmed statistically and never instantaneously, and only locally at the scales associated with wavenumbers within the inertial subrange, and the latter exists only for isotropic turbulence and at high Reynolds numbers. Moreover, since the dissipation of the generalized SGS turbulent kinetic energy is, by definition, positive, the assumption of local balance

implies that also the production of generalized SGS turbulent kinetic energy is positive. However, the assumption that the production is always positive implies that the energy transfer always occurs from the largest to the smallest scales and prevents positive transfers of kinetic energy from the subgrid scales to the resolved ones (backscatter). Since the energy exchange processes between the resolved and unresolved scales generally occur in both directions (forward scatter and back scatter), as has been observed by various authors [10], the assumption that the production of generalized SGS turbulent kinetic energy is always positive does not enable the complexity of the energy exchange processes which characterize the turbulence to be adequately taken into account.

The third inconsistency of the dynamic models concerns the calculation of the above mentioned Smagorinsky coefficient  $C_s$ . It is calculated with variational methods, (e.g. with a least squares minimization method [11] or Lagrangian method [4]). These methods identify a single value of the scalar coefficient  $C_s$  from a system of five independent scalar equations relating the components of the anisotropic part of the generalized SGS turbulent stress tensor to the components of the resolved strain-rate tensor. This procedure does not provide completely acceptable results. Moreover, when simulating confined flows at high Reynolds number, the results of the dynamic procedure are of doubtful reliability in the region close to the wall including both the viscous sublayer and the buffer layer [12]. In this region, the filter width used in the dynamic procedure is larger than most eddies that govern the momentum and energy transfer. Consequently, the dynamic procedure used under these conditions for the calculation of the coefficient  $C_s$  is not able to fully account for the local subgrid dissipative processes that affect the entire domain.

In this paper the main drawbacks of the large eddy simulation models present in literature are overcome and a new LES model is proposed. The closure relation for the generalised SGS turbulent stress tensor: a) complies with the principle of turbulent frame indifference [13]; b) takes into account both the anisotropy of the turbulence velocity scales and turbulence length scales; c) removes any balance assumption between the production and dissipation of SGS turbulent kinetic energy. In the proposed model: a) the closure coefficient which appears in the closure relation for the generalised SGS turbulent stress tensor is theoretically and uniquely determined without adopting Germano's dynamic procedure; b) the generalised SGS turbulent stress tensor is related exclusively to the generalised SGS turbulent kinetic energy (which is calculated by means of its balance equation) and the modified Leonard tensor. The calculation of the viscous dissipation is carried out by integrating its balance equation. The closure relations (which intervene in the above mentioned viscous dissipation equation) are formulated in such a way that the modeled equation respects the form invariance and frame dependence of the exact equation.

For the simulation of the unsteady three-dimensional turbulent flow it is very important to control the dissipation produced by the numerical scheme. The numerical dissipation removes energy from the dynamically important small-scale eddies; for this reason unsteady, three-dimensional turbulent simulations are much less tolerant of numerical dissipation [14]. On the other hand the numerical scheme must be accurate. Morinishi et al. [14] proposed a staggered fourth order finite difference scheme. Vasilyev [15] showed that the extension of the scheme, suggested by Morinishi et al., to non uniform meshes produces a fourth order accurate finite difference scheme that is not fully conservative. In this paper the numerical integration of the filtered equations is performed by the staggered fourth order finite difference scheme proposed by Morinishi et al.

## 2 The turbulence model

According to Bardina's scale similarity assumption, the generalized SGS turbulent stress tensor can be expressed by

$$\tau_{ij} = (1+r)L_{ij}^m \quad (1)$$

where  $r$  is an unknown scalar coefficient and  $L_{ij}^m$  is the modified Leonard tensor.

In this paper it is demonstrated that, starting from the scale similarity assumption in (1), (by simple mathematical calculations) a closure relation is reached for the generalized SGS turbulent stress tensor, in which there appears no coefficient to be calibrated or to be calculated dynamically, and which is given by the following relation:

$$\tau_{ij} = \left( \frac{2E}{L_{kk}^m} \right) L_{ij}^m \quad (2)$$

It is easy to verify that as, by definition, the generalized SGS turbulent kinetic energy equal to half the trace of the generalized SGS turbulent stress tensor [17],

$$E = \frac{\tau_{kk}}{2} \quad (3)$$

from Equation (1) is obtained

$$\tau_{kk} = (1+r)L_{kk}^m \quad \text{where} \quad r = \frac{2E - L_{kk}^m}{L_{kk}^m} \quad (4)$$

Introducing (4) into (1) gives:

$$\tau_{ij} = \left( 1 + \frac{2E - L_{kk}^m}{L_{kk}^m} \right) L_{ij}^m = \left( \frac{2E}{L_{kk}^m} \right) L_{ij}^m \quad (5)$$

The closure relation (5) is obtained without any assumption of local balance between the production and dissipation of generalized SGS turbulent kinetic energy and may thus be considered applicable to LES with the filter width falling into the range of wave numbers greater than the wave number corresponding to the maximum turbulent kinetic energy. The closure relation (5) for the generalized SGS turbulent stress tensor: a) complies with the principle of turbulent frame indifference given that it relates only objective tensors; b) takes into account both the anisotropy

of the turbulence velocity scales and turbulence length scales; c) assumes scale similarity; d) guarantees an adequate energy drain from the grid scales to the subgrid scales and guarantees backscatter; e) overcomes the inconsistencies linked to the dynamic calculation of the closure coefficient used in the modelling of the generalized SGS turbulent stress tensor.

The generalized SGS turbulent kinetic energy,  $E$ , is calculated by solving its balance equation, defined by the following equation:

$$\frac{DE}{Dt} = -\frac{1}{2} \frac{\partial \tau(u_k, u_k, u_m)}{\partial x_m} - \tau_{mk} \frac{\partial \bar{u}_k}{\partial x_m} - \frac{\partial \tau(p, u_m)}{\partial x_m} + \nu \frac{\partial^2 E}{\partial x_m \partial x_m} + \tau(F_{ok}, u_k) - \nu \tau \left( \frac{\partial u_k}{\partial x_m}, \frac{\partial u_k}{\partial x_m} \right) \quad (6)$$

The 1st and 3rd terms of the right-hand side of Equation (6) express the turbulent diffusion of the generalized SGS turbulent kinetic energy:

$$\frac{1}{2} \frac{\partial \tau(u_i, u_i, u_k)}{\partial x_k} + \frac{\partial \tau(p, u_k)}{\partial x_k} = \frac{\partial (F_E)_k}{\partial x_k} \quad (7)$$

The following equation is used for the calculation of  $(F_E)_k$

$$(F_E)_k = D \sqrt{E} \bar{\Delta} \frac{\partial E}{\partial x_k} \quad (8)$$

Scalar coefficient  $D$  is dynamically calculated by means of a Germano identity applied to the 1st and 3rd terms on the right-hand side of Equation (6)

$$(F_E^T)_k - \overline{(F_E)_k} = \frac{1}{2} T(u_i, u_i, u_k) - \frac{1}{2} \overline{\tau(u_i, u_i, u_k)} + T(p, u_k) - \overline{\tau(p, u_k)} \quad (9)$$

where the first term on the left-hand side of Equation (9) is the turbulent diffusion of the generalized SGS turbulent kinetic energy at the test level, the symbol  $\overline{(\cdot)}$  indicates the filter operation at the test level and

$$T(f, g) = \overline{f g} - \overline{f} \overline{g} \quad (10)$$

$$T(f, g, h) = \overline{f g h} - \overline{f} \overline{g h} - \overline{g} \overline{f h} - \overline{h} \overline{f g} - \overline{f} T(g, h) - \overline{g} T(f, h) - \overline{h} T(f, g) \quad (11)$$

are, respectively, the generalized second and third order central moment at the test level [16]. According to (10) and (11), Equation (9) reads

$$(F_E^T)_k - \overline{(F_E)_k} = \frac{1}{2} \overline{u_i u_i u_k} - \frac{1}{2} \overline{u_i} \overline{u_i} \overline{u_k} - \frac{1}{2} \overline{u_k} \overline{\tau(u_i, u_i)} + \frac{1}{2} \overline{u_k} \tau(u_i, u_i) - \overline{u_i} \overline{\tau(u_i, u_k)} + \overline{u_i} \tau(u_i, u_k) + T(p, u_k) - \overline{\tau(p, u_k)} \quad (12)$$

Using Equation (8), the left-hand side term of Equation (9) takes the form

$$(F_E^T)_k - \overline{(F_E)_k} = D \sqrt{E^T} \bar{\Delta}^T \frac{\partial E^T}{\partial x_k} - D \sqrt{E} \bar{\Delta} \frac{\partial E}{\partial x_k} \quad (13)$$

where  $E^T$  is the generalized SGS turbulent kinetic energy at the test level. The coefficient  $D$  is calculated by introducing (13) into (12).

The last term on the right-hand side of Equation (6) is defined as viscous dissipation:

$$\varepsilon = \nu \tau \left( \frac{\partial u_i}{\partial x_j}, \frac{\partial u_i}{\partial x_j} \right) \quad (14)$$

In the proposed LES model a further balance equation is introduced for the subgrid viscous dissipation  $\varepsilon$ . This equation, expressed in terms of the generalized central moments, takes the form [17]:

$$\begin{aligned} & \frac{\partial \varepsilon}{\partial t} + \frac{\partial \bar{u}_k \varepsilon}{\partial x_k} - \nu \frac{\partial^2 \varepsilon}{\partial x_k \partial x_k} + \nu \frac{\partial}{\partial x_k} \tau \left( u_k, \frac{\partial u_i}{\partial x_j}, \frac{\partial u_i}{\partial x_j} \right) + \\ & 2\nu \frac{\partial}{\partial x_k} \left( \frac{\partial \bar{u}_i}{\partial x_j} \tau \left( u_k, \frac{\partial u_i}{\partial x_j} \right) \right) + 2\nu \frac{\partial}{\partial x_k} \tau \left( \frac{\partial u_k}{\partial x_i}, \frac{\partial p}{\partial x_i} \right) - \\ & 2\nu \frac{\partial}{\partial x_k} \left( \frac{\partial \bar{u}_i}{\partial x_j} \frac{\partial \tau_{ik}}{\partial x_j} \right) + 2\nu \tau \left( \frac{\partial u_i}{\partial x_k}, \frac{\partial u_k}{\partial x_j}, \frac{\partial u_i}{\partial x_j} \right) + \\ & 2\nu \frac{\partial \bar{u}_k}{\partial x_j} \tau \left( \frac{\partial u_i}{\partial x_k}, \frac{\partial u_i}{\partial x_j} \right) + 2\nu \frac{\partial \bar{u}_i}{\partial x_k} \tau \left( \frac{\partial u_k}{\partial x_j}, \frac{\partial u_i}{\partial x_j} \right) + \\ & 2\nu \frac{\partial \bar{u}_i}{\partial x_j} \tau \left( \frac{\partial u_i}{\partial x_k}, \frac{\partial u_k}{\partial x_j} \right) + 2\nu \frac{\partial \tau_{ik}}{\partial x_j} \frac{\partial^2 \bar{u}_i}{\partial x_j \partial x_k} + \\ & 2\nu^2 \tau \left( \frac{\partial^2 u_i}{\partial x_j \partial x_k}, \frac{\partial^2 u_i}{\partial x_j \partial x_k} \right) - 2\nu \tau \left( \frac{\partial u_i}{\partial x_j}, \frac{\partial F_{oi}}{\partial x_j} \right) = 0 \end{aligned} \quad (15)$$

In this paper an original expression is proposed for the “modeled” form of the balance equation for the generalized SGS turbulent kinetic energy dissipation, in which the unknown tensors are modeled by adopting the hypothesis of scale similarity and Equation (15) takes the form:

$$\begin{aligned} & \frac{\partial \varepsilon}{\partial t} + \frac{\partial \bar{u}_k \varepsilon}{\partial x_k} - \nu \frac{\partial^2 \varepsilon}{\partial x_k \partial x_k} + \frac{\partial}{\partial x_k} C_{F_\varepsilon} \frac{E^2}{\varepsilon} \frac{L_{kl}^m}{L_{jj}^m} \frac{\partial \varepsilon}{\partial x_l} + \\ & 2\nu \frac{\partial}{\partial x_k} \left( \frac{\partial \bar{u}_i}{\partial x_j} \left( \frac{C_{F_\varepsilon} E}{\varepsilon} \frac{\partial \varepsilon}{\partial x_q} \delta_q \tau \left( \frac{\partial \bar{u}_i}{\partial x_n}, \frac{\partial \bar{u}_n}{\partial x_n} \right) \right) \right) - \\ & 2\nu \frac{\partial}{\partial x_k} \left( \frac{\partial \bar{u}_i}{\partial x_j} \frac{\partial}{\partial x_j} \left( \frac{2E}{L_{qq}^m} L_{ik}^m \right) \right) - C_{P_\varepsilon} \frac{\varepsilon (-L_{ij}^m \bar{S}_{ij})}{L_{kk}^m} + \\ & 2\nu \frac{\partial \bar{u}_k}{\partial x_j} \frac{\varepsilon}{\tau} \tau \left( \frac{\partial \bar{u}_i}{\partial x_k}, \frac{\partial \bar{u}_i}{\partial x_j} \right) + 2\nu \frac{\partial \bar{u}_i}{\partial x_k} \frac{\varepsilon}{\tau} \tau \left( \frac{\partial \bar{u}_k}{\partial x_j}, \frac{\partial \bar{u}_k}{\partial x_j} \right) + \\ & 2\nu \frac{\partial \bar{u}_i}{\partial x_j} \frac{\varepsilon}{\tau} \tau \left( \frac{\partial \bar{u}_i}{\partial x_k}, \frac{\partial \bar{u}_i}{\partial x_j} \right) + 2\nu \frac{\partial \bar{u}_i}{\partial x_k} \frac{\varepsilon}{\tau} \tau \left( \frac{\partial \bar{u}_k}{\partial x_j}, \frac{\partial \bar{u}_k}{\partial x_j} \right) + \end{aligned}$$

$$2\nu \frac{\partial \bar{u}_i}{\partial x_j} \frac{\varepsilon}{\tau} \left( \frac{\partial \bar{u}_i}{\partial x_k}, \frac{\partial \bar{u}_k}{\partial x_j} \right) + 2\nu \frac{\partial}{\partial x_j} \left( \frac{2E}{L_{mm}^m} L_{ik}^m \right) \frac{\partial^2 \bar{u}_i}{\partial x_j \partial x_k} + \tau \left( \frac{\partial \bar{u}_q}{\partial x_s}, \frac{\partial \bar{u}_s}{\partial x_q} \right) \quad (16)$$

$$C_{D_\varepsilon} \frac{\varepsilon^2}{E} = 0$$

where  $\delta_i = (1,1,1)$  and in which the closure coefficients are calculated dynamically by means of the Germano identities. For the simulation of the unsteady three-dimensional turbulent flow it is very important to control the dissipation produced by the numerical scheme. The numerical dissipation removes energy from the dynamically important small-scale eddies; for this reason unsteady, three-dimensional turbulent simulations are much less tolerant of numerical dissipation [14]. On the other hand the numerical scheme must be accurate. In this paper the numerical integration of the filtered equations is performed by the staggered fourth order finite difference scheme proposed by Morinishi et al. [14]. As it is shown by Vasilyev [15], the extension of the scheme suggested in [14] to non-uniform meshes produce a fourth order accurate finite difference scheme that is not fully conservative.

Let  $y$  be the non-uniform direction with point distribution  $y_j$ . The following difference operator, with stencil  $n$  acting on the generic quantity  $\phi$  with respect to  $y$ , is used

$$\frac{\delta_n \phi}{\delta_n y} \Big|_{y_j} \equiv \frac{\phi(y_{j+n/2}) - \phi(y_{j-n/2})}{y_{j+n/2} - y_{j-n/2}},$$

and the following interpolation operator is given by

$$\bar{\phi}^{ny} \Big|_{y_j} \equiv \frac{(y_j - y_{j-n/2})\phi(y_{j+n/2}) + (y_j - y_{j+n/2})\phi(y_{j-n/2})}{y_{j+n/2} - y_{j-n/2}}$$

Let  $NS4$  be the difference between the exact convective term and its discrete approximation. The fourth order accurate scheme for the divergence form of the convective term is given by:

$$\frac{\partial u_j u_i}{\partial x_j} - NS4 \equiv \frac{9}{8} \frac{\delta_1}{\delta_1 x_j} \left[ \left( \frac{9}{8} \bar{U}_j^{1x_i} - \frac{1}{8} \bar{U}_j^{3x_i} \right) \bar{U}_i^{1x_j} \right] - \frac{1}{8} \frac{\delta_3}{\delta_3 x_j} \left[ \left( \frac{9}{8} \bar{U}_j^{1x_i} - \frac{1}{8} \bar{U}_j^{3x_i} \right) \bar{U}_j^{1x_i} \right] \quad (17)$$

This numerical scheme has good conservation properties and fourth order accuracy and enables the integration of the filtered momentum equation and of the filtered SGS kinetic energy and viscous dissipation balance equations.

### 3 Result and discussion

Turbulent channel flows (between two flat parallel plates placed at a distance of  $2L$ ) are simulated with the proposed Large Eddy Simulation model at different friction-velocity-based Reynolds numbers ( $Re^*$ ), ranging from 395 to 2340.

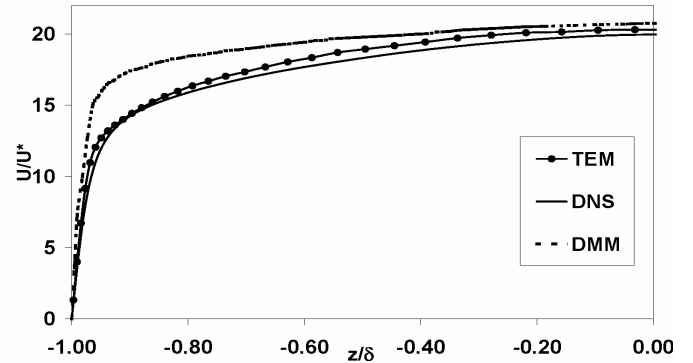


Fig. 1. Time-averaged streamwise velocities. Comparison between DNS and LES results obtained with DMM and the proposed model (TEM). Channel flow,  $Re^* = 395$ .

In order to validate the proposed closure relation for the generalized SGS turbulent stress tensor, the numerical results obtained with the proposed model are compared with DNS results [18] and with experimental data [19].

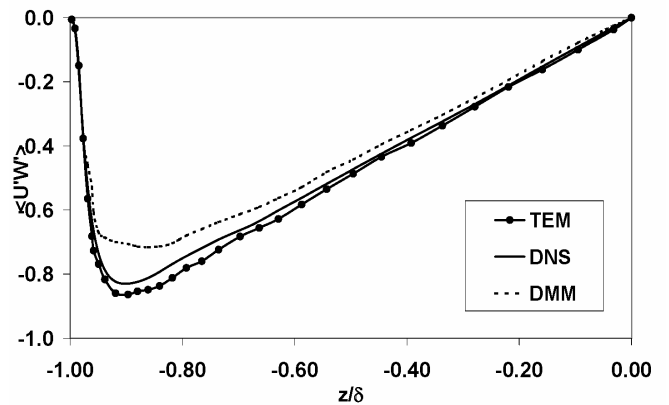


Fig. 2. Reynolds stress  $\langle u_1' u_3' \rangle$ . (indexes (1) and (3) denote, respectively the streamwise and wall-normal directions) Comparison between DNS and LES results obtained with the dynamic mixed model (DMM) and the proposed model (TEM). Channel flow,  $Re^* = 395$ .

In Figure 1 is plotted the profile of the time-averaged streamwise velocity component obtained with the proposed model compared with the profile obtained with DNS [18] and the Dynamic Mixed Model, DMM [2], for channel flow at  $Re^* = 395$ . The figure shows that the profile obtained with the proposed model agrees more the DNS velocity profile than with the profile obtained with the DMM, both in the boundary layer and in the region inside the channel.

Figure 2 shows the profiles of the component  $\langle u_1' u_3' \rangle$  of the Reynolds stress tensor, (where indexes 1 and 3 denote, respectively, the streamwise and wall-normal directions), obtained from the simulations carried out with the proposed

model compared with the profiles of the analogous component obtained from DNS and from simulations carried out with the DMM, at  $Re^* = 395$ . As can be seen from figure 2, the profile of the component  $\langle u_1'u_3' \rangle$  calculated with the proposed model yields a similar profile to that of the corresponding component of the Reynolds stress tensor obtained by the DNS, whilst the DMM provides values which are greatly underestimated.

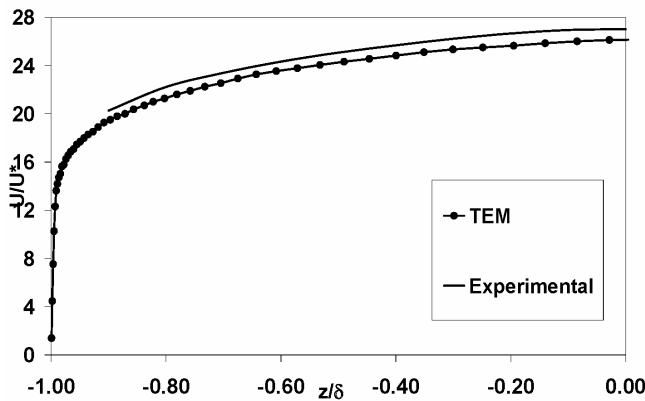


Fig. 3. Time-averaged streamwise velocities. Comparison between experimental measurements and LES results obtained with the proposed model (TEM). Channel flow,  $Re^* = 2340$ .

Figure 3 shows the profile of the time-averaged streamwise velocity component for a channel flow at  $Re^* = 2340$  obtained with the proposed model compared with the profile of the analogous velocity component measured experimentally [19]. The agreement between the two velocity profiles is very good. Figure 4 compares the profile of the component  $\langle u_1'u_3' \rangle$  of the Reynolds stress tensor calculated with the proposed model with the profile of the similar component of the Reynolds stress tensor obtained from experimental measurements [19], for a channel flow at  $Re^* = 2340$ .

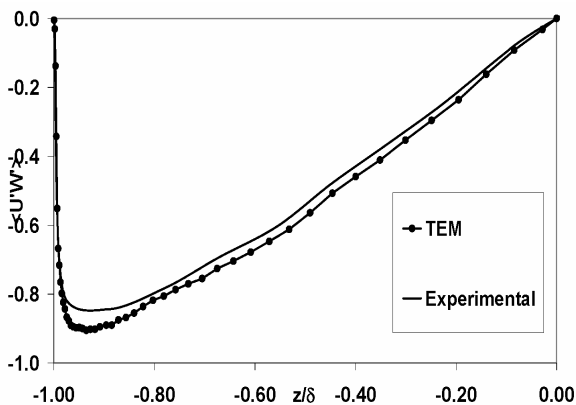


Fig. 4. Reynolds stress  $\langle u_1'u_3' \rangle$ . Comparison between experimental measurements and LES results obtained with the proposed model (TEM). Channel flow,  $Re^* = 2340$ .

Figure 4 shows that at  $Re^* = 2340$  the proposed model provides a profile of the component  $\langle u_1'u_3' \rangle$  in agreement with that of the corresponding component of the Reynolds stress tensor obtained from the experimental measurements.

Figures 5 and 6 show the profiles of the various terms of the balance equation of the generalized SGS turbulent kinetic energy  $E$  (production term:  $P_E$ ; turbulent transport term:  $T_E$ ; convection term:  $C_E$ ; viscous diffusion term  $D_E$ ; viscous dissipation:  $\epsilon$ ), calculated with this model and averaged over time and over homogeneous planes, plotted in terms of the distance from the wall (expressed in wall units,  $z^+$ ), for channel flow at  $Re^*$  of 395 and 1655, respectively.

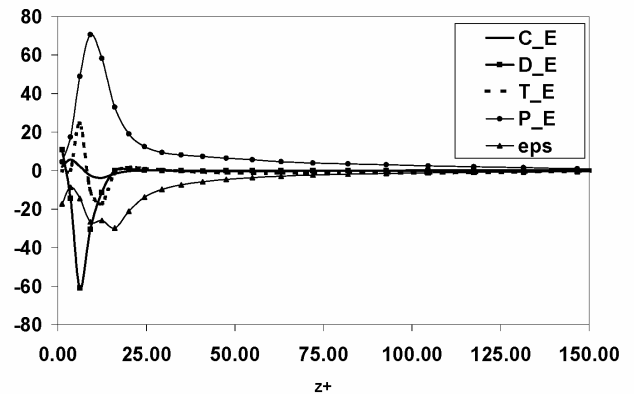


Fig. 5. Generalized SGS turbulent kinetic energy balance terms averaged over time and over homogeneous planes. Production:  $P_E$ ; Turbulent transport:  $T_E$ ; Convection:  $C_E$ ; Viscous diffusion:  $D_E$ ; Viscous dissipation :  $\epsilon$ . Channel flow,  $Re^*=395$ .

Figure 7 shows instantaneous profiles of the terms of the balance equations of  $E$  averaged over homogeneous planes, for channel flow at  $Re^* = 2340$ . Figure 5, 6 and 7 demonstrate that the balance between production and dissipation of the generalizes SGS turbulent kinetic energy is confirmed only in a limited region between the buffer layer and the log layer ( $20 < z^+ < 40$ ) whilst it is not confirmed in other regions of the domain.

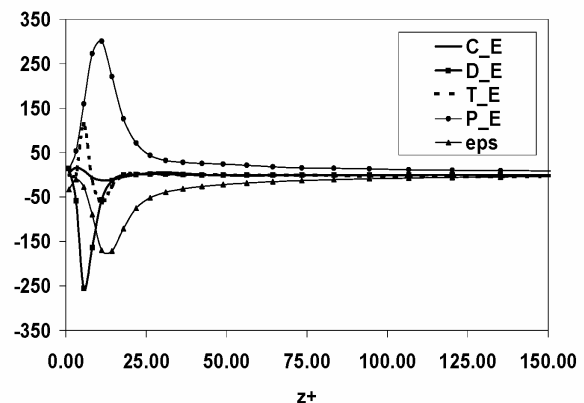


Fig. 6. Generalized SGS turbulent kinetic energy balance terms averaged over time and homogeneous planes. Production:  $P_E$ ; Turbulent transport:  $T_E$ ; Convection:  $C_E$ ; Viscous diffusion:  $D_E$ ; Viscous dissipation:  $\epsilon$ . Channel flow,  $Re^*=1655$ .

The viscous dissipation of  $E$  is balanced in the viscous sublayer ( $z^+ < 5$ ) by the viscous diffusion term whilst the production of  $E$  is practically negligible. Moving away from the wall, in the first part of the buffer layer, the production term of  $E$  increases until reaching its maximum value ( $z^+ \approx$

10) and the terms of turbulent transport and viscous diffusion of  $E$  are comparable with the production term of  $E$ . In the region between the buffer layer and the log layer ( $20 < z^+ < 40$ ) the convective and turbulent transport terms and the viscous diffusion term are negligible compared with the production and dissipation terms.

Only in this limited region there is a balance between the production and the dissipation of  $E$ . towards the center of the channel ( $z^+ > 30$ ) the viscous dissipation tends towards a minimum but not negligible value. In this region the production term of  $E$  is balanced not only by the dissipation but also by the turbulent transport of  $E$ .

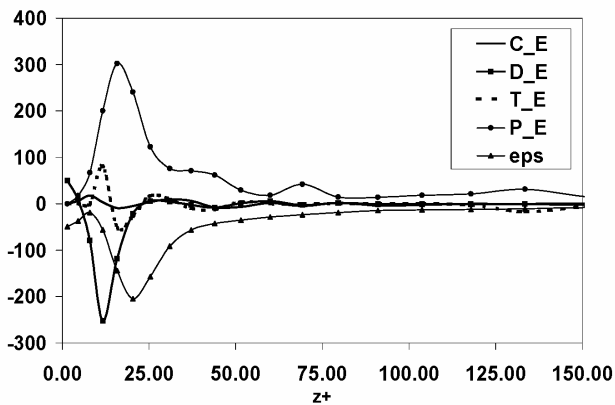


Fig. 7. Instantaneous generalized SGS turbulent kinetic energy balance terms averaged over homogeneous planes. Production:  $P_E$ ; Turbulent transport:  $T_E$ ; Convection:  $C_E$ ; Viscous diffusion:  $D_E$ ; Viscous dissipation:  $\epsilon$ . Channel flow,  $Re^*=2340$ .

#### 4 Conclusion

In this paper a new LES model is proposed. The proposed closure relation for the generalized SGS turbulent stress tensor: complies with the principle of turbulent frame indifference; takes into account both the anisotropy of the turbulence velocity scales and turbulence length scales; removes any balance assumption between the production and dissipation of SGS turbulent kinetic energy. In the proposed model the generalized SGS turbulent stress tensor is related exclusively to the generalized SGS turbulent kinetic energy (which is calculated by means of its balance equation) and the modified Leonard tensor. The filtered momentum equations are solved by using a staggered fourth order finite difference scheme. The proposed model is tested for a turbulent channel flow at Reynolds numbers (based on friction velocity and channel half-width) ranging from 395 to 2340.

#### References:

[1] M. Germano, U. Piomelli, P. Moin, W.H. Cabot, A dynamic subgrid scale eddy viscosity model. *Phys. Fluids*, A3, 1991, pp. 1760-1765.

[2] Y. Zang, R.L. Street, J.R. Koseff, A dynamic mixed subgrid-scale model and its application to turbulent recirculating flows, *Physics of Fluids*, A 5, 1993, pp. 3186-3196.

[3] B. Vreman, B. Geurts, H. Kuerten, On the formulation of the dynamic mixed subgrid-scale model, *Physics of Fluids*, 6, 1994, pp. 4057-4059.

[4] C. Meneveau, T.S. Lund, W.H. Cabot, A Lagrangian dynamic subgrid-scale model of turbulence. *J. Fluid Mech*, 319, 1996, pp. 353-385

[5] V.M. Salvetti, V.M. S. Banerjee, A priori tests of a new dynamic subgrid-scale model for finite difference large-eddy simulations, *Phys. Fluids*, 7, 1995, pp. 2831-2847.

[6] B. Tao, J. Katz, C. Meneveau, Geometry and scale relationships in high Reynolds number turbulence determined from three-dimensional holographic velocimetry, *Phys. Fluids*, 12, 2000, pp. 941-944.

[7] K. Tennekes, J.L. Lumley, *A first course in turbulence*, MIT Press, 1972

[8] A.S. Monin, A.M. Yaglom, *Statistical Fluid Mechanics: Mechanics of Turbulence*, MIT Press, 1972.

[9] C.G. Speziale, T.B. Gatski, Analysis and modelling of anisotropies in the dissipation rate of turbulence, *J Fluid Mech*, 344, 1997, pp. 155-180.

[10] U. Piomelli, W.H. Cabot, P. Moin, S. Lee, Subgrid-scale backscatter in turbulent and transitional flows, *Phys. Fluids*, A3, 1991, pp.1766-1771.

[11] D.K. Lilly, A proposed modification of the Germano subgrid scale closure method, *Phys. Fluids*, A4, 1992, pp. 633-635.

[12] F. Sarghini, U. Piomelli, E. Balaras, Scale-similar models for large-eddy simulation, *Phys. Fluids*, 11, 1999, pp. 1596-1607.

[13] K. Hutter, K. Joenk, *Continuum Methods of Physical Modeling*, Springer, 2004.

[14] Y. Morinishi, T.S. Lund, O. Vasilyev, P. Moin, Fully Conservative Higher Order Finite Difference Schemes for Incompressible Flow, *Journal of Computational Physics*, 143, 1998, pp. 90-124.

[15] O. Vasilyev, High Order Finite Difference Schemes on Non-uniform Meshes with Good Conservation Properties, *Journal of Computational Physics*, 157, 2000, pp. 746-761.

[16] M. Germano, Turbulence: the filtering approach, *Journal of Fluid Mechanics*, 238, 1992, pp. 323-336.

[17] F. Gallerano, E. Pasero, G. Cannata, A dynamic two-equation Sub Grid Scale model, *Continuum Mechanics and Thermodynamics*, Vol. 17, No 2, 2005, pp. 101-123.

[18] N.N. Mansour, R.D. Moser, J. Kim, Fully developed turbulent channel flow simulation, *AGARD Advisory Report*, 343.

[19] G. Comte-Bellott, High Reynolds number channel flow experiment, *AGARD Advisory Report*, 343.